# Gas-sensor properties of SnO$_2$ films implanted with gold and iron ions

K. NOMURA
*School of Engineering, The University of Tokyo, Hongo 7-3-1, Bunkyo-ku, Tokyo 113, Japan*

H. SHIOZAWA, T. TAKADA
*New Cosmos Electric Co. Ltd, Mitsuya-naka, 2-5-4, Yodogawa-ku, Osaka 432, Japan*

H. REUTHER, E. RICHTER
*Forshungszentrum Rossendorf e.V., Institut fur Ionenstrahlphysik und Materialforschung, D-01314 Dresden, Germany*

SnO$_2$ gas-sensor films were modified by implantation of gold and iron ions. The change in electrical resistivity of the films caused by inflammable gases, H$_2$, CO, CH$_4$ and C$_2$H$_5$OH, was measured in the temperature range 100–500 °C, and compared to non-implanted films. The morphological changes caused by gold and iron ion implantation were also investigated by atomic force microscopy. After ion implantation and annealing at 600 °C, the sensitivity to H$_2$ and CO gas was found to increase, and the dynamic range of the sensitivity to ethanol was improved. The sensitivity to CH$_4$ was low before and after ion implantation. Fe$_2$O$_3$ (3%SnO$_2$) film was also modified by gold ion implantation for comparison.

## 1. Introduction

Tin oxide (SnO$_2$) has the electrical properties of an n-type semiconductor, and has been used as a gas sensor based on its conductivity changes produced by the oxidation and reduction of adsorbed or absorbed gases. Many types of SnO$_2$-based gas sensors have been developed since 1962 [1], but their responses are affected by the various preparation methods. Most typical sensor materials are prepared by chemical treatment of SnO$_2$ with a catalyst such as platinum [2] and palladium [3]. We have previously studied gas-sensor properties of SnO$_2$ based films prepared by spray pyrolysis [4], and have found that the sensitivity increased with the addition of p-type nickel and manganese oxides together with palladium catalyst. We also confirmed from $^{119}$Sn Mössbauer spectra that the change in the chemical states of tin oxides, when exposed to inflammable gases (H$_2$, CO, and CH$_4$), depends on the kinds of additive oxides [5] and that Mössbauer parameters of Sn(IV) oxides change drastically in coincidence with the temperature, which specifies the gas-sensing function [6, 7].

The development of a highly selective CO gas sensor is desired to detect incomplete combustion, the early stages of fires and to prevent accidental asphyxiation. For example, Au/α-Fe$_2$O$_3$(Ti) [8], Au–MgO/SnO$_2$ (Sb) [9] and Au–LaO$_3$/SnO$_2$ [10] sensors have been developed for CO detection. The doping effect of gold is of great interest.

On the other hand, there are only a few studies on the application of ion implantation to the development of an SnO$_2$-based gas sensor [11]. Chemical preparations by spray pyrolysis and coprecipitation are simple for mixing other oxides, but it is difficult to exclude anions such as Cl$^-$ ions. An ion-implantation technique enables the development of a well-characterized and integrated compact device. Ion implantation can dope any ion to a certain depth from the top surface, and make multilayers with different carrier density with the addition of a catalytic ion.

In this work, we attempted to modify SnO$_2$ films by doping with gold and iron ions using an ion-implantation technique, and studied the electrical responses against inflammable gases, H$_2$, CO, CH$_4$, and C$_2$H$_5$OH, before and after ion implantation and annealing.

## 2. Experimental procedure

Tin oxide films with the thickness of 500 nm and 100 nm were prepared on heating Al$_2$O$_3$ substrates (300 °C) by an electron-beam evaporation method using an SnO$_2$ pellet, and were further annealed in air at 600 °C for 1 h. A tin oxide film gas sensor is shown in Fig. 1, which is composed of comb-like platinum electrodes for gas detection and heater electrodes on the rearside. The gap between the electrodes is 0.05 mm and the total width is 9 mm. The films were modified by implantation with 40 keV Au ions ($4 \times 10^{15}$ ions cm$^{-2}$) and 57 keV Fe ions ($1.1 \times 10^{16}$ ions cm$^{-2}$). All implanted films were again later annealed at 600 °C in ambient air. It was estimated by a TRIM program [12] that the doped ions were located within

the top 100 nm thickness, and this was confirmed by measurement of depth profiles with Auger electron spectroscopy. The electrical resistance of the film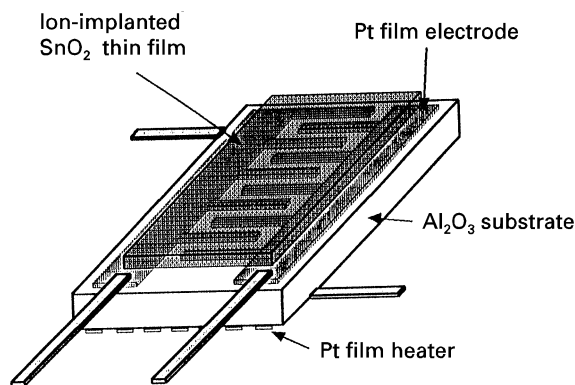s was measured in the range 100–500 °C in air containing 1000 p.p.m. $CH_4$, CO, or $H_2$, air containing 20 p.p.m. ethanol, and also dry air. Gas sensitivity is defined as the ratio, $R_a/R_g$, of the resistance measured in dry air, $R_a$, to the resistance in air containing gas, $R_g$. The grains of some $SnO_2$ films and $Fe_2O_3$ films were observed using an atom force microscope (AMF, Rasterscope TM 3000, DME).



*Figure 1* Schematic drawing of the electrode for tin oxide-based film gas sensor production.

## 3. Results and discussion

### 3.1. Effect of ion implantation on $SnO_2$ films, 500 nm thick

The gas sensitivity of $SnO_2$ films (500 nm thick) before and after implantation of iron and gold ions and annealing for 1 h is shown in Fig. 2. The maximum sensitivities of $SnO_2$ film annealed for 1 h before implantation were 8.4 for $H_2$, 3.4 for CO, 10.2 for ethanol and 1.3 for $CH_4$ at 400 °C. It showed a high response for each gas except $CH_4$. When the $SnO_2$ film was implanted with only iron ions (energy 57 keV, dose
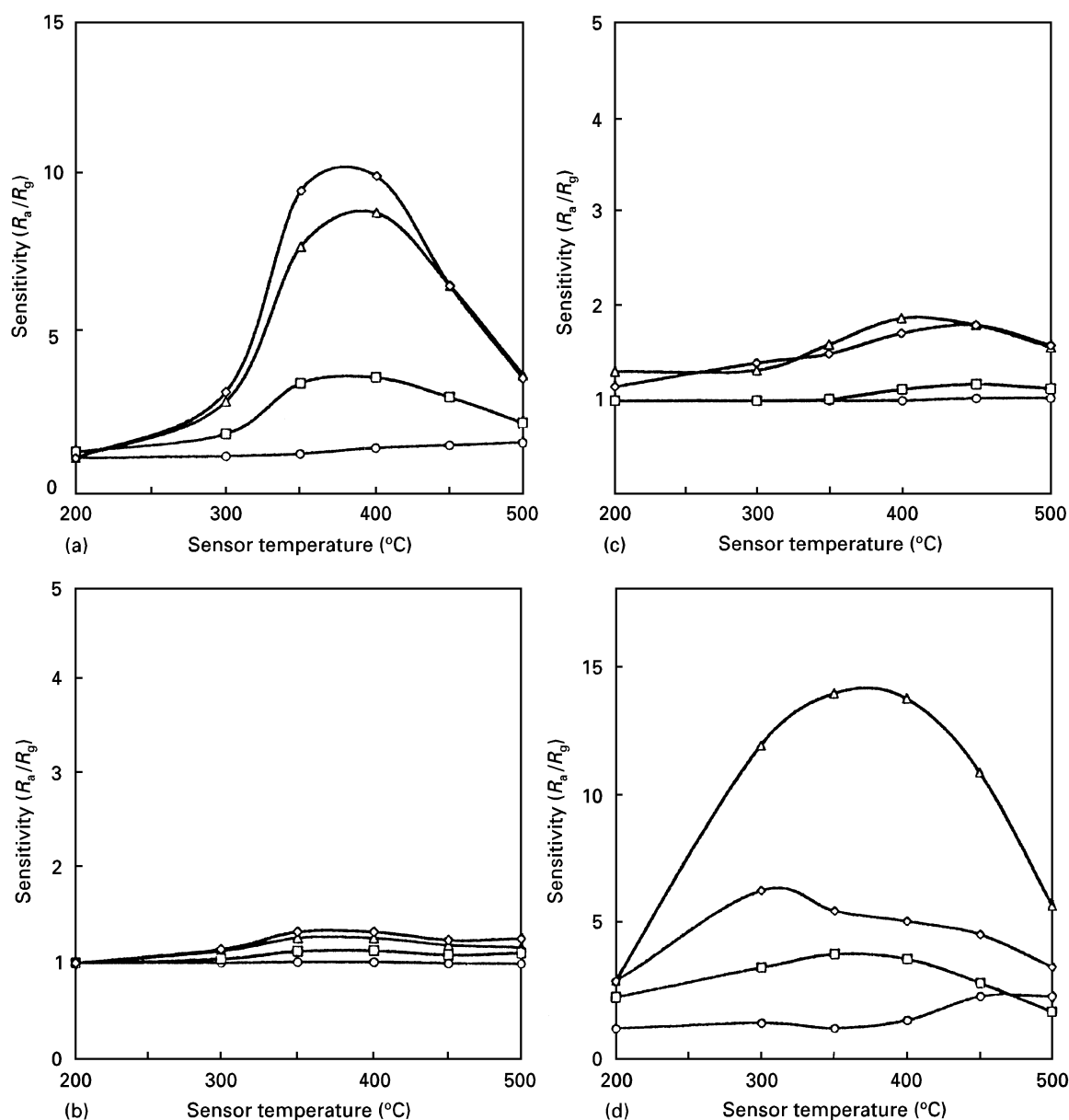


*Figure 2* Gas sensitivity of $SnO_2$-based films (500 nm thick): (a) unimplanted and annealed at 600 °C for 1 h; (b) implanted with iron ions $(1.1 \times 10^{16}$ ions cm$^{-2})$; (c) implanted with iron ions $(1.1 \times 10^{16}$ ions cm$^{-2})$; and gold ions $(4 \times 10^5$ ions cm$^{-2})$: (d) implanted with iron and gold ions, and annealed at 600 °C for 1 h. (○) $CH_4$, (△) $H_2$, (□) CO, all 1000 p.p.m.; (◇) $C_2H_5OH$, 20 p.p.m.
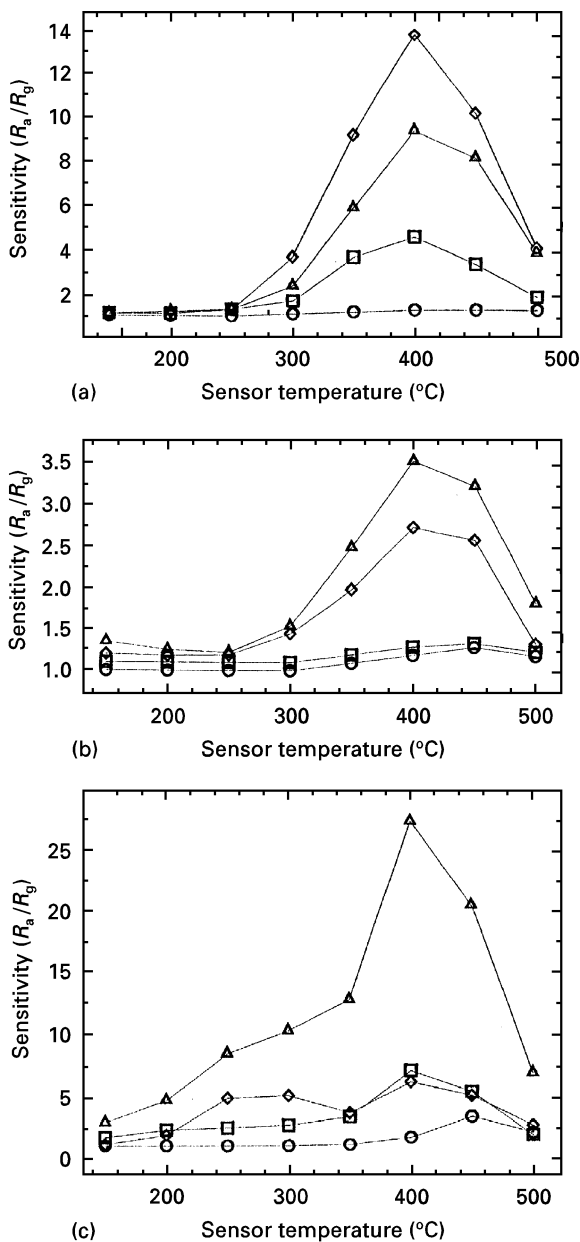
Figure 3 Gas sensitivity of tin oxide-based films (500 nm thick), annealed at 600 °C for 2 h: (a) unimplanted; (b) implanted with iron ions; and (c) implanted with iron and gold ions. (○) $CH_4$, (△) $H_2$, (□) CO, all 1000 p.p.m.; (◇) $C_2H_5OH$, 20 p.p.m.
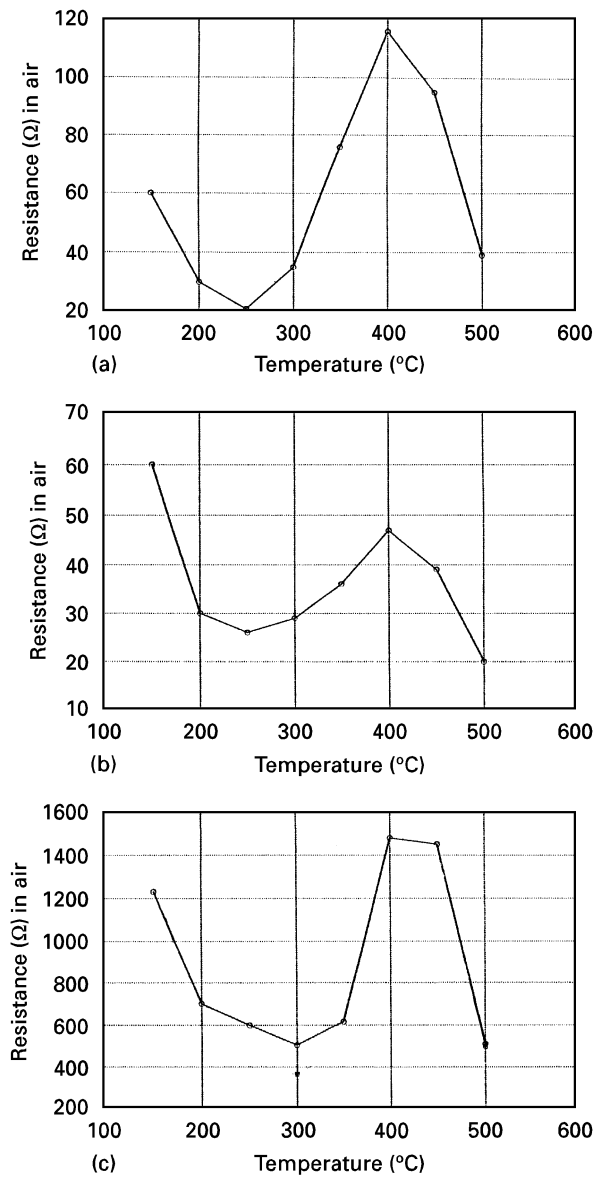


Figure 4 Temperature dependence of electrical resistance of tin oxide-based films (500 nm thick), annealed at 600 °C for 2 h in air; (a) unimplanted; (b) implanted with iron ions; and (c) implanted with iron and gold ions.

$1.1 \times 10^{16}\,cm^{-2}$), the sensitivity to $H_2$, CO and ethanol also decreased to less than 1.35, as shown in Fig. 2b. When the films of iron-doped $SnO_2$ were further implanted with gold ions ($4 \times 10^{15}\,cm^{-2}$), the sensitivity to $H_2$ and ethanol gases increased slightly (Fig. 2c). The implanted samples without annealing showed a decreased sensitivity for each gas. However, when further annealed for 1 h in ambient air, the sensitivity increased (especially for $H_2$), whereas the sensitivity was limited to about half that of pure $SnO_2$ film for low concentrations of ethanol (Fig. 2d). The implanted tin oxides without annealing in air had an unstable response to each gas and did not show high sensitivity. This is probably due to the production of oxygen vacancies by preferential sputtering of oxygen near the surface by the implantation process [13] and the production of unstable valence states in the implanted ions.

When these samples were annealed for a further hour, as shown in Fig. 3, an increase in the sensitivity together with a slight shift to higher temperature, was observed. In the case of pure $SnO_2$ film, the increase by annealing for a further hour was up to about 1.4 times for all gases, whereas in iron- and gold-doped $SnO_2$ films it was about twice that, for $H_2$ and CO gases. The sensitivity to ethanol was not increased as much by additional annealing.

Fig. 4 shows the temperature dependence of the electrical resistance of tin oxides with and without iron and gold ions. The base resistance of $SnO_2$ film did not change significantly by doping with iron ions although the peak resistance at 400 °C became smaller. This means the partial blocking or extinction of the active sites for absorption/adsorption of oxygen. The grains became smaller after iron-ion implantation, but the change in grains was estimated to be limited within one-fourth of $SnO_2$ layers with 500 nm thickness,

303

which corresponds to the location of iron ions in the $SnO_2$ layer, as shown in Fig. 5. Iron ions are considered to be not perfectly incorporated in the $SnO_2$ crystal. If the $Fe^{3+}$ was incorporated into the $SnO_2$, the carrier electrons would have decreased, and as a result, its resistance would have increased.

On the other hand, when iron and gold ions were implanted together, the electrical resistance of the film was about ten times higher than that of a non-doped film, and the sensitivity to $H_2$ and CO increased. It is clear from the results shown in Figs 3 and 4 that the degree of the sensitivity to $H_2$ and CO is related to the relative height of the resistance peak observed at 300–400 °C in air. This suggests that the chemically absorbed oxygens in surface and subsurface layers of oxides are released easily by the reaction with $H_2$ or CO at temperatures higher than 300 °C. The removal of adsorbed oxygen results in a reduction of the potential barrier at the surface and an increase in the carrier density by releasing the carrier electrons back into tin oxide matrix. Iron- and gold-ion implantation and post-annealing increase the number of active sites for detection of $H_2$ and CO gases.
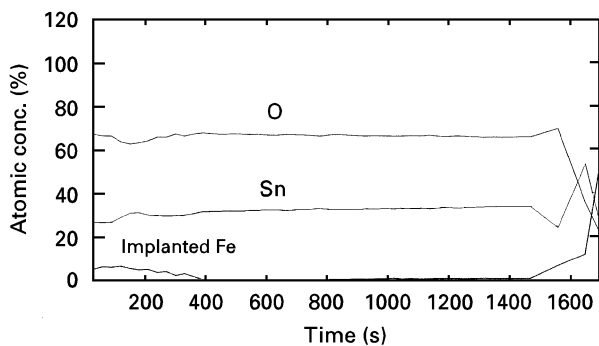


*Figure 5* Depth profile of $SnO_2$ (500 nm) films, implanted with iron ions and annealed at 600 °C for 1 h, by Auger electron spctroscopy. Implantation energy = 57 eV.
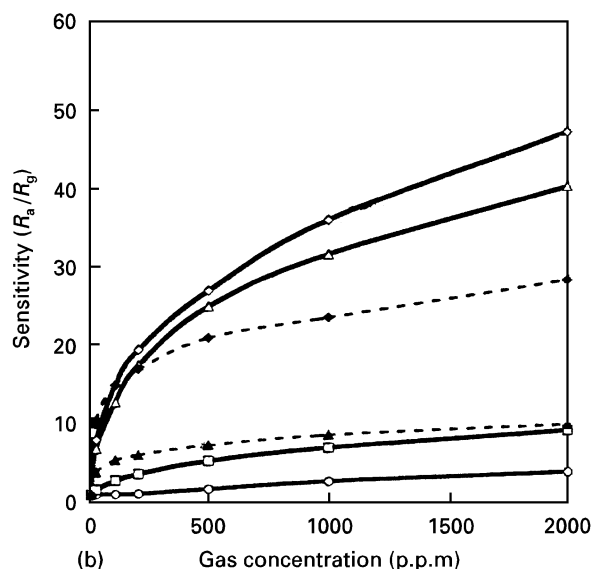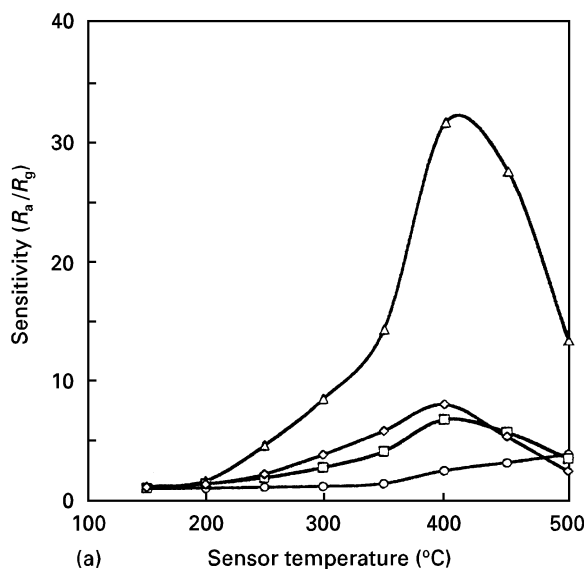
The temperature and gas-concentration dependencies of the sensitivity are shown in Fig. 6 for the $SnO_2$ films with and without iron and gold ions, annealed for 24 h at 600 °C. The sensitivity increased over a wider range of gas concentration for the $SnO_2$ films doped with iron and gold ions, whereas the sensitivity of an undoped $SnO_2$ film had a tendency to saturate at higher gas concentrations. This suggests that the smaller grains produced by iron and gold-ion implantation are not seriously merged by annealing. Therefore, the small grains produced by ion implantation and annealing contribute to the increase of the gas sensitivity, as well as the electrical resistance. This is probably caused by a charge compensation of $Fe^{3+}$ as well as a morphology change.

## 3.2. Effect of ion implantation of $SnO_2$ with 100 nm thickness

Gold or iron ions were implanted on thin $SnO_2$ films to confirm whether implanted gold itself had a catalytic effect. When gold ions were implanted in $SnO_2$ film with 100 nm thickness, the sensitivities at 400 °C for $H_2$, CO and ethanol were 4.8, 1.6 and 2.6, respectively, whereas the sensitivities of the iron-ion implanted $SnO_2$ films were less than 1.5 for all gases. Fig. 7 shows AFM images of non-implanted, iron-ion implanted, and gold-ion implanted $SnO_2$ films. The grain boundary became obscure after iron-ion implantation, and the small grains could be observed in the films implanted with gold ions. The grains did not grow so much on annealing.

When a tin oxide film was covered with gold (thickness < 10 nm) by a sputtering method, no resistance peak was observed in the temperature range between 300 and 500 °C, and no response to any gas was obtained. This means that there are no active sites for oxygen adsorption/absorption on the surface in this temperature range. However, when the tin oxide film
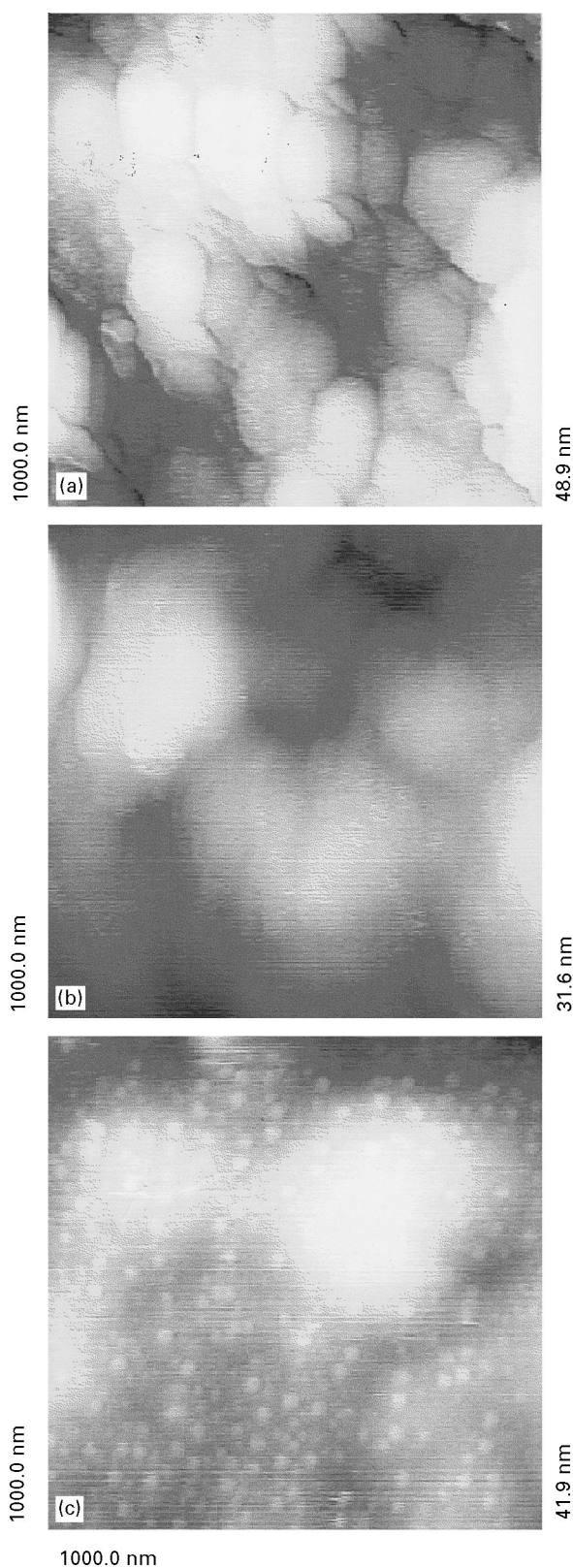


*Figure 6* Gas sensitivity of $SnO_2$-based film (500 nm thick), implanted with iron and gold ions and annealed at 600 °C for 24 h: (a) temperature dependence of gas sensitivity (CH$_4$, ($\square$) CO, and $\triangle$ H$_2$: 1000 p.p.m.), ($\diamond$ C$_2$H$_5$OH: 20 p.p.m.), (b) relationship of gas sensitivity to gas concentration at an operating temperature of 400 °C: ($\bigcirc$) CH$_4$; ($\triangle$) H$_2$; ($\square$) CO, ($\diamond$) C$_2$H$_5$OH; (--$\blacktriangle$--) H$_2$, unimplanted; (--$\blacklozenge$--) C$_2$H$_5$OH unimplanted.

*Figure 7* AFM images of $SnO_2$ (100 nm) films: (a) unimplanted; (b) iron-ion implanted; and (c) iron and gold-ion implanted.

covered by gold was further implanted with iron ions and annealed, the gas sensitivity appeared (the highest was 4 for $H_2$), although the response was unstable. It is considered that the thin gold film is damaged by iron-ion bombardment, and that some oxides on the top surface appear after annealing in air. The increase in sensitivity probably results not only from the re-appearance of oxides on the surface by iron-ion implantation, but also from the interaction of iron oxides and bombarded gold particles. Kobayashi *et al.* [8] reported that the catalytic effect of gold appeared at 350 °C due to the fine particles used when chemically mixing gold into iron oxides.

### 3.3. Effect of ion implantation of $Fe_2O_3$ film with 100 nm thickness

In order to consider the previous results in more detail, we prepared iron oxide films with 100 nm thickness by an electron-beam evaporation method using a 3 wt % $SnO_2$-doped iron oxide pellet. Then gold ions were implanted on the iron oxide films at the same energy and dose as used previously. The sensitivity obtained decreased unexpectedly for CO gas detection, as shown in Fig. 8. The selectivity for $H_2$ gas detection increased relatively at 300 °C. The grains of iron oxide changed little after gold ion implantation. It has also been reported that a change in surface morphology is caused by ion bombardment, and that the compaction increases with increasing ion mass and dose through the series, argon, krypton and xenon [14]. The surface change induced by gold-ion implantation was larger than by iron-ion implantation. The decrease in the sensitivity is probably due to damaged and sputtered oxides on the surfaces, which could not be readily recovered by annealing, because the tin oxide film was too thin.

The thick $SnO_2$ films (500 nm) implanted with iron and gold ions are composed of two layers; a deep layer of pure $SnO_2$ and a surface layer of $SnO_2$ doped with gold and iron ions. The relative increase of gas sensitivity for $H_2$ and CO may be partially due to the small grains produced on the surface of the thick films by the gold-ion implantation, and the decrease of gas sensitivity for ethanol due to the diffusion control of ethanol through the compacted top layer. Stedile *et al.* reported that the O/Sn ratio reached up to 1.9 even on annealing an $SnO_2$ film implanted with iron ions at 400 °C for 1.5 h [11]. It was found that the insensitive layers of an $SnO_2$ surface induced by ion implantation can be recovered by post-annealing at 600 °C for at least 2 h, and that thick $SnO_2$ films are required for ion implantation. Iron- and gold-ion implanted tin oxides showed a high resistance, which is caused by a morphological change of tin oxides, as well as by a charge compensation of $Fe^{3+}$ doping.

### 4. Conclusion

The initial purpose to increase considerably the selectivity and the sensitivity only for CO could not be accomplished by implantation of gold and iron ions in $SnO_2$-based gas sensors. However, it was found that the sensitivity to $H_2$, ethanol, and CO was enhanced in a wide range of gas concentrations by ion implantation and post-annealing, and that the annealing at 600 °C in air was effective to recover the active oxygen sites.

It was found, as secondary results, that iron oxide films doped with tin oxide have the potential to detect $H_2$ and CO gas with high sensitivity, and that the
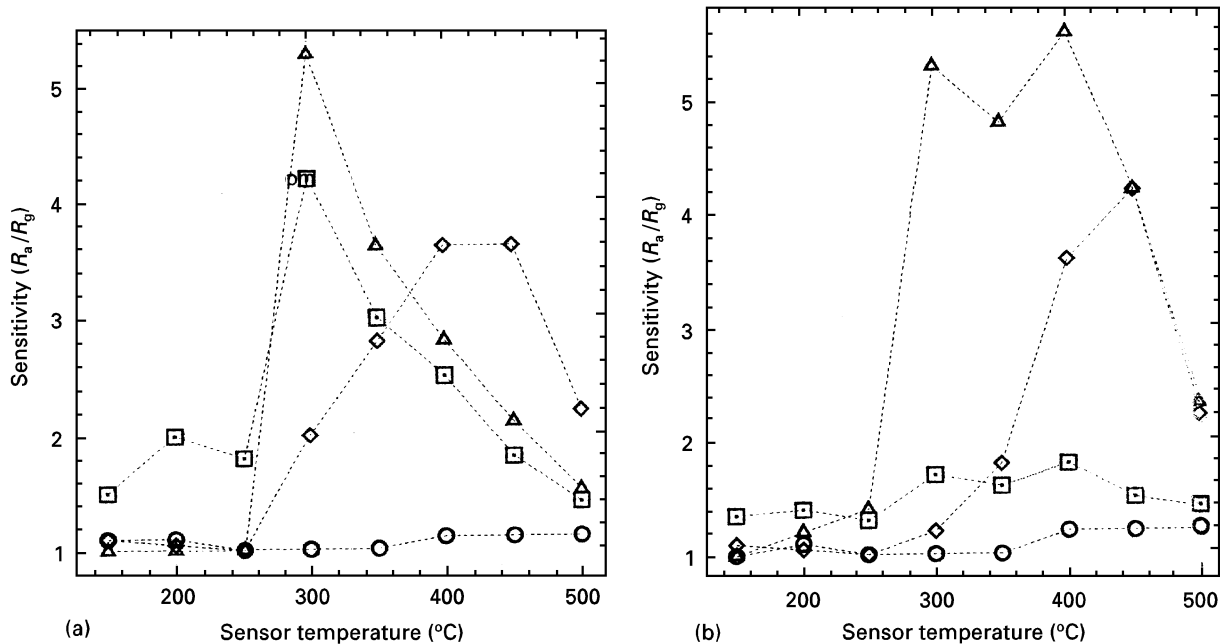
*Figure 8* Gas sensitivity of iron oxides (3% $SnO_2$) films (100 nm thick) (a) before implantation, and (b) after implantation with gold ions and annealing at 600 °C for 1 h. ($\bigcirc$) $CH_4$, ($\triangle$) $H_2$, ($\square$) CO, all 1000 p.p.m.; ($\diamond$) $C_2H_5OH$, 20 p.p.m.

selectivity for $H_2$ gas becomes relatively high at 300 °C after gold-ion implantation because the active sites for CO and ethanol were suppressed by the gold-ion implantation.

Iron- and gold-ion implantations induce damage in crystalline $SnO_2$ films, but a proper post-annealing enables the gas sensor properties to be recovered.

## References
1. N. TAGUCHI, Jpn Pat. S45-38200 (1970).
2. Y. OKAYAMA, H. FUKAYA, K. KOJIMA, Y. TERASAWA and T. HANDA, in "Proceedings of the International Meeting on Chemical Sensors", edited by T. Seiyama, K. Fueki, J. Shiokawa and S. Suzuki, Fukuoka, Japan, September 1983, (Elsevier, Amsterdam–Oxford–New York–Tokyo, 1983) pp. 29–34.
3. N. MURAKAMI, Y. MATSUURA, K. TAKAHATA and K. IHOKURA, in "Proceedings of the 2nd International Meeting on Chemical Sensors", edited by J. L. Aucouturier, J. S. Cauhapé, M. Destriau, P. Hagenmuller, C. Lucat, F. Ménil, J. Portier and J. Salardenne, Bordeaux, France, July 1986, (Bordeaux Chemical Sensors, Bordeaux, 1986), pp. 268–9.
4. K. NOMURA, Y. UJIHIRA, S. S. SHARMA, A. FUEDA and T. MURAKAMI, *J. Mater. Sci.* **24** (1989) 937.
5. S. S. SHARMA, K. NOMURA, and Y. UJIHIRA, *ibid.*
6. *Idem, J. Appl. Phys.* **71** (1992) 2000.
7. K. NOMURA, S. S. SHARMA and Y. UJIHIRA, *Nucl. Instrum. Meth. Phys. Res.* **B76** (1993) 357.
8. T. KOBAYASHI, M. HARUTA, H. SANO and M. NAKANE, *Sensors Actuators* **13** (1988) 339.
9. T. KOBAYASHI, M. HARUTA and H. SANO, *Chem. Express* **4** (1989) 217.
10. K. FUKUI and M. NAKANE, in "Proceedings of the 5th International Meeting on Chemical Sensors", edited by A. D'Amico and C. DiNatale, Rome, 11–14th July, 1994 (Elsevier Science, Lausanne, 1995) p. 620.
11. F. C. STEDILE, C. V. BARROS LEITE, W. H. SCHRIEINER and I. J. R. BAUMVOL, *Thin Solid Films* **190** (1990) 139.
12. J. F. ZIEGLER, J. P. BIERSACK and U. LITTMARK, "The Stoppings and Range of Ions and Solids", (Pergamon, New York, 1985).
13. G. B. BARBI, J. P. SANTOS, P. SERRINI, N. GIBSON, M. C. HORRILLO and L. MANES, in "Proceedings of the 5th International Meeting on Chemical Sensors," edited by A. D'Amico and C. DiNatale, Rome, 11–14th, July, 1994 (Elsevier Science, Lausanne, 1995) p. 715.
14. S. P. KAYE, H. KHEYRANDISH and J. S. COLLIGON, *Nucl. Instrum. Meth. Phys. Res.* **B61** (1991) 380.